



ELSEVIER

Available online at www.sciencedirect.com

Proceedings of the Combustion Institute xxx (2009) xxx–xxx

**Proceedings
of the
Combustion
Institute**www.elsevier.com/locate/proci

Relationships between composition and pulmonary toxicity of prototype particles from coal combustion and pyrolysis[☆]

Seung-Hyun Cho^a, Jong-Ik Yoo^a, Audrey T. Turley^a,
C. Andrew Miller^a, William P. Linak^{a,*}, Jost O.L. Wendt^b,
Frank E. Huggins^c, M. Ian Gilmour^d

^a National Risk Management Research Laboratory, U.S. Environmental Protection Agency, E305-01,
Research Triangle Park, NC 27711, USA

^b Department of Chemical Engineering, University of Utah, Salt Lake City, UT 84112, USA

^c Consortium for Fossil Fuel Science, Department of Chemical and Materials Engineering,
University of Kentucky, Lexington, KY 40506, USA

^d National Health and Environmental Effects Research Laboratory, U.S. Environmental Protection Agency,
Research Triangle Park, NC 27711, USA

Abstract

The hypothesis that health effects associated with coal combustion fly-ash particles are exacerbated by the simultaneous presence of iron and soot was tested through two sets of experiments. The first set created prototype particles from complete and partial combustion, or oxygen free pyrolysis of a high iron Illinois bituminous coal in an externally heated drop-tube furnace. The second experiment created prototype particles consisting of iron and soot in various concentrations from doped ethylene Burke–Schumann flames. Size-classified samples from the coal tests were separated into coarse (>2.5 μm), fine (0.5–2.5 μm) and ultrafine (<0.5 μm) fractions, and analyzed for total carbon, elemental composition, and detailed iron and sulfur speciation. In a similar manner, ultrafine particles from the ethylene flame tests were also analyzed for total carbon and elemental composition. Pulmonary inflammatory responses were determined after intratracheal aspiration of 100 μg samples in female CD1 mice. IL-6 and neutrophil responses were monitored as markers of inflammation. With carbon present, the coal data suggested that the ultrafine particles containing soot were more toxic than fine or coarse particles containing char, even though the iron and sulfur speciation varied only slightly with particle size. Iron and sulfur chemistry were, however, dependent on the extent of carbon burnout achieved. In the absence of carbon, ultrafine particles (high in bisulfates and semi-volatile alkali metals) were *less* toxic than the fine fraction (high in oxidized iron and sulfates). Iron-soot particles created from ethylene flames were more toxic than an equivalent physical mixture of iron oxide and soot, and the toxicity depended primarily on the soot concentration. However, taken as

[☆] Prepared for presentation at: 32nd International Symposium on Combustion, McGill University, Montreal, Canada, August 3–8, 2008.

* Corresponding author. Fax: +1 919 541 0554.

E-mail address: linak.bill@epa.gov (W.P. Linak).

whole, these data do not support the notion that iron and soot interact to enhance pulmonary inflammatory responses.

© 2009 Published by Elsevier Inc. on behalf of The Combustion Institute.

Keywords: Coal fly-ash; Pyrolysis residue particles; Soot; Ultrafine particles; Health effects

1. Introduction

Epidemiological data have suggested a link between adverse health effects and particles containing transition metals, including iron [1]. Toxicological studies have also suggested a link between inhalation of particles containing transition metals and oxidative stress in lung cells [2–4] and it has been postulated that inhalation of coal combustion fly-ash particles causes oxidative stress [5] because of the presence of iron [6]. Furthermore, iron is present in atmospheric particles from cities including St. Louis [7], where increased mortality has been attributed to levels of PM_{2.5} [8]. Subsequently, it was suggested from *in vitro* studies that ferric iron in an aluminosilicate glass phase served as the source of bio-available iron from coal fly-ash [9], and that the process to make iron bio-available depended on ash particle size [10]. Kennedy and co-workers have further investigated particle toxicity of ultrafine iron and soot aerosol from ethylene gas diffusion flames and concluded that oxidative stress resulted from a *synergistic interaction* between soot and iron [11,12]. They also found that soot burnout mechanisms often resulted in the formation of mixed iron-soot particles, and iron oxide particles largely separate from soot.

In a previous paper, we found a link between coal ash toxicity and carbon in the ash for a range of coals burned in a variety of combustion equipment [13]. In these experiments, only two ultrafine samples contained significant amounts of carbon thought to be soot. This is consistent with reports by Veranth et al. [14] indicating over a third of the carbon in fly-ash is present as soot, and that this is affected by the application of combustion modifications for NO_x control. Coal ash particulate matter is emitted with a size distribution containing three modes: a vaporization mode (containing particles denoted as ultrafine, <0.5 μm), a fine fragmentation mode (fine, 0.5–2.5 μm) and a coarse fragmentation mode (coarse, >2.5 μm) [15]. The vaporization mode contains, and is often enriched in, volatile and semi-volatile components, including sulfur and metals, which have vaporized in the flame and subsequently nucleated. Any carbon found in this fraction would most likely be in soot form [14]. Previous X-ray absorption fine structure (XAFS) spectroscopy analysis showed the sulfur on particles containing soot is present enriched in thiophenic forms [13]. The two fragmentation modes have similar bulk

mineral compositions, including silicates, although they may be coated with condensed or reacted semi-volatile metals, such as arsenic and selenium [16], while most of the carbon mass likely consists of unburned char. Although one might suspect that the vaporization mode might be the most toxic, previous work suggests that the fine fragmentation mode may also have toxic effects. The objective of this study was to test the hypothesis that particles from coal combustion cause lung injury due to the simultaneous presence of iron and carbon. Experiments were conducted on a single high iron content coal that allowed systematic variations of carbon content in the particles emitted. These tests involved various degrees of carbon burnout, including a pyrolysis condition with little or no carbon burnout. These experiments produced ultrafine samples with ~8% iron and low (nearly zero) carbon, ~2% iron and 80% carbon, and <0.5% iron and 95% carbon. The coal tests were complemented by studies on soot particles containing iron from ethylene diffusion flames. These latter experiments, similar to those conducted by Kennedy and co-workers [11,12], were designed to complement the coal ash toxicity tests by using similar toxicological markers for both fuels. They also allow for independent control, over a wider range, on the amounts of iron and carbon in the samples.

2. Materials and methods

2.1. Generation and collection of size-classified coal combustion and pyrolysis particles

Nine size-classified pulverized coal residue particle samples were generated using a three-zone, programmable bench-scale (1 g/h) drop-tube furnace. For this study, a single high iron, high sulfur Illinois bituminous coal was used. The coal was burned in such a manner as to produce particles with no (or very low) carbon, medium carbon, and very high carbon (under pyrolysis conditions). In each case, particles were size-classified into coarse, fine, and ultrafine fractions. Table 1 provides the proximate, ultimate, and elemental analyses of this coal. Details regarding the furnace are provided elsewhere [13]. All three furnace zones were maintained at 1350 °C. Flow rates of the annular and transport gases (air or nitrogen) were maintained at 12.0 and 0.5 L/min, respectively, resulting in a calculated Reynolds number

Table 1
Q3 Analysis of Illinois bituminous coal (as received)

Proximate analysis (%)		Mineral analysis (%)	
Moisture	16.99	SiO ₂	54.60
Ash	9.29	Fe ₂ O ₃	18.93
Volatile	33.89	Al ₂ O ₃	13.90
Fixed carbon	39.85	CaO	4.31
		SO ₃	4.18
		K ₂ O	1.50
<i>Ultimate analysis (%)</i>		Na ₂ O	1.48
Carbon	59.00	TiO ₂	0.78
Hydrogen	4.32	MgO	0.71
Nitrogen	1.19	P ₂ O ₅	0.11
Chlorine	0.17	MnO ₂	0.06
Sulfur	3.11	BaO	0.04
Oxygen ¹	5.96	SrO	0.03
¹ By difference			
HHV (MJ/kg)	5.04	<i>Sulfur forms (%)</i>	
		Pyritic	1.23
		Sulfate	<0.01
		Organic	1.87

140 and residence time within the alumina reactor of
141 approximately 340 and 2 s. From the furnace exit,
142 the combustion gases and residue particles, at a
143 flow of 12.5 L/min and at 80 °C to eliminate water
144 condensation, were directed to a five-stage cas-
145 cade cyclone (Thermo Electron Corp.) to collect
146 particles greater than approximately 0.5 μm diam-
147 eter [17]. Ultrafine particles (here defined as
148 <0.5 μm diameter) were collected on 47 mm poly-
149 carbonate membrane filters located immediately
150 after the cyclone. Once collected, the cyclone
151 catches were combined to yield fine (0.5–2.5 μm)
152 and coarse (>2.5 μm) particle samples.

153 The oxidizing environment within the drop-
154 tube furnace was varied to control the amount
155 of carbon in the particle samples. This was accom-
156 plished by sequentially substituting nitrogen for
157 first the annular air and then both the annular
158 and transport air. Thus, the first set of experi-
159 ments were performed using air for both the annu-
160 lar and transport flows and this produced an
161 overall extremely lean stoichiometric ratio (SR)
162 of ~115. The second set of experiments used air
163 for the transport flow and nitrogen for the annu-
164 lar flow and produced an overall SR ~ 4.6. How-
165 ever, oxygen diffusion from the transport flow
166 likely produced an effective local SR much less
167 than 4.6 in the vicinity of the coal particles and
168 this resulted in only partial oxidation and signifi-
169 cant unburned carbon in the ash. Finally, the
170 third set of experiments used nitrogen for both
171 flows producing pyrolysis in the complete absence
172 of oxygen (SR ~ 0).

173 2.2. Generation and collection of iron-soot particles 174 from ethylene Burke–Schumann flames

175 Three additional samples containing varying
176 ratios of iron and carbon (soot) were generated

177 using an ethylene-fueled Burke–Schumann co-
178 annular laminar diffusion burner following
179 designs of Santoro et al. [18]. Iron was added to
180 the ethylene fuel using vaporized ferrocene with
181 the relationship between the vapor pressure of fer-
182 rocene in ethylene and temperature, between 4
183 and 87 °C, provided by Jacobs et al. [19] The fer-
184 rocene vaporization system followed a design by
185 Zhang and Megaridis [20]. The ethylene and over
186 ventilated air flow rates for these experiments
187 were 0.188 and 55.8 L/min, respectively. The eth-
188 ylene was further adjusted to control the iron con-
189 centration in the resulting soot.

190 Particle emissions were sampled and collected
191 on 47 mm polycarbonate membrane and 47 mm
192 quartz fiber filters for subsequent chemical and
193 toxicological analysis. Particle size analysis using
194 a Scanning Mobility Particle Sizer (TSI Inc.,
195 model 3080/3022A) confirmed that these particles
196 were all ultrafine (<0.5 μm). The three experi-
197 mental conditions produced soot particles without
198 iron (0% Fe), low iron (2.6% Fe), and high iron
199 (13.3% Fe). Without iron addition, the ethylene
200 soot produced a unimodal particle size distribu-
201 tion with a mean diameter of ~95 nm. As iron
202 (a known soot oxidation catalyst) is added the
203 mass emissions are notably reduced. Iron reduced
204 the 95 nm mode, but produced bimodal behavior
205 with the addition of a 25 nm mode.

206 2.3. Chemical characterization of size-classified 207 particles

208 Samples between 500 and 1000 mg were
209 needed for the multiple analyses which, depend-
210 ing on the combustion condition, required up to sev-
211 eral weeks to collect. As expected, the medium
212 and high carbon coal samples and soot only ethyl-
213 ene samples were easier to collect (higher mass
214 emission rates) than the zero carbon and iron-soot
215 samples. All samples were analyzed by wavelength
216 dispersive X-ray fluorescence (WD-XRF) spec-
217 troscopy [21]. Knowing the sample mass, the
218 WD-XRF software can quantify elements with
219 atomic numbers ≥9 (fluorine). For fly-ash sam-
220 ples the most stable metal oxide was assumed.
221 Other (unidentified) sample mass was initially
222 reported as unknown. For these samples the
223 unknown sample component was subsequently
224 positively identified to be carbon using a Sunset
225 Laboratory Inc. analyzer (model 107 A). The car-
226 bon analysis based on thermal optical transmit-
227 tance, provided information on total carbon and
228 the partitioning between organic carbon (OC)
229 and elemental carbon (EC).

230 The coal residue samples were also analyzed by
231 the element-specific techniques, ⁵⁷Fe Mössbauer
232 and XAFS spectroscopies. Mössbauer spectro-
233 scopy was conducted for the coal particle samples
234 using a Halder Mössbauer (model 351) driving
235 system operating in the symmetric (triangular

236 wave) constant acceleration mode. Iron Möss-
237 bauer spectra were accumulated for up to 10 days
238 and analyzed using combinations of quadrupole
239 (two peak) and magnetic (six peak) absorption
240 units based on a Lorentzian peak shape. Sulfur
241 XAFS spectra were collected for the same samples
242 at beamline X-19A of the National Synchrotron
243 Light Source (NSLS), Brookhaven National Lab-
244 oratory, NY. Additional details of XAFS experi-
245 mentation are described elsewhere [22]. Initial
246 analysis of sulfur XAFS spectra followed conven-
247 tional data reduction practice; least-square fitting
248 for the sulfur X-ray absorption near edge (XANE)
249 spectra [23,24] was then performed to quantify the
250 distribution of sulfur among the different forms.

251 2.4. Toxicological characterization of the coal and 252 iron-soot particles

253 Pulmonary instillation studies were carried out
254 in female CD1 mice to compare the relative toxic-
255 ity of all samples gathered from both the coal fed
256 drop-tube furnace and the ethylene flame. Briefly,
257 the mice were anesthetized with isoflurane and
258 instilled via involuntary aspiration with 100 μg
259 of particles suspended in 50 μL of sterile saline.
260 The size-classified particle suspensions in saline
261 were sonicated and then vigorously vortex-mixed
262 immediately before instillation in an attempt to
263 minimize particle agglomeration. Four or eighteen
264 hours later, mice were euthanized and the lungs
265 were cannulated via the trachea and lavaged with
266 three volumes of sterile saline. The lung washes
267 were analyzed for interleukin-6 (IL-6) and neutro-
268 phils (polymorphonuclear leukocytes, PMNs) as
269 markers of pulmonary inflammation. Additional
270 animals were instilled with saline to produce base-
271 line control data or lipopolysaccharide (LPS) as a
272 pro-inflammatory positive control.

273 3. Results and discussion

274 3.1. Samples examined

275 Nine particle samples from the complete combus-
276 tion, partial combustion, and oxygen free
277 pyrolysis of the Illinois coal were obtained and
278 divided into three groups based on carbon burn-
279 out. The first group represented particles obtained
280 under high excess air conditions ($\text{SR} \sim 115$) to
281 eliminate all but trace quantities of carbon in the
282 sampled particles (denoted as “zero carbon”).
283 Unlike the medium and high carbon samples, it
284 was possible to close the elemental mass balance
285 for the zero carbon samples using only the XRF
286 results. Carbon analysis of these samples indi-
287 cated EC amounts always at blank levels and
288 OC amounts that sometimes varied slightly above
289 blank levels. The second group of tests produced
290 prototype particles from coal combustion at

291 $\text{SR} \sim 4.6$, that contained moderate amounts of
292 carbon (denoted as “medium carbon”). The third
293 group of tests produced prototype particles from
294 coal pyrolysis with no oxygen ($\text{SR} \sim 0$), and pro-
295 duced particles containing all the residual (fixed)
296 carbon with zero burnout (denoted as “high car-
297 bon”). Each group contained each of the three size
298 classifications (coarse, fine, and ultrafine parti-
299 cles). Using the iron-doped ethylene diffusion
300 flame three ultrafine particulate samples were pro-
301 duced with iron concentration of 0% (100% soot),
302 2.6% (96.3% soot), and 13.3% (81.0% soot). These
303 were augmented by two additional samples con-
304 sisting of (1) 100% $\gamma\text{-Fe}_2\text{O}_3$ nanoparticles (Nano-
305 structured and Amorphous Materials Inc.); and
306 (2) a physical mixture the $\gamma\text{-Fe}_2\text{O}_3$ nanoparticles
307 and flame-formed soot (15.8% Fe). The form of
308 $\gamma\text{-Fe}_2\text{O}_3$ was chosen because previous work [13]
309 had shown this form of iron to be identified with
310 coal ultrafine particles.

311 3.2. Elemental compositions

312 Figure 1 shows the elemental composition of
313 each of the size-classified zero carbon, medium
314 carbon and high carbon (pyrolysis residue) parti-
315 cle samples, as well as for the five ethylene flame
316 related samples (all with diameters $<0.5 \mu\text{m}$).
317 For the zero carbon particles, the coarse and fine
318 fragmentation size classes had similar composi-
319 tions, except for iron which was enriched in the
320 fine particles. The source of this iron enrichment
321 in the fine fragmentation mode is consistent with
322 a hypothesized size range of extraneous pyrites,
323 which here contained half of the total coal sulfur
324 (Table 1). As expected, the ultrafine particles were
325 rich in semi-volatile alkali metals but also con-
326 tained appreciable calcium and iron. Consistent
327 with surface condensation/reaction mechanisms,
328 sulfur was present in increasing amounts as the
329 particle size decreased.

330 The medium carbon particle samples contained
331 appreciable amounts of carbon (50–80%). It is
332 reasonable to assume that the form of carbon in
333 the ultrafine fraction is soot, while the large
334 amounts of carbon in the larger particles sug-
335 gested the presence of char in both the fine and
336 the coarse (fragmentation mode) fractions. The
337 inorganic compositions of the fine and coarse
338 fractions were similar, while the ultrafine fraction
339 was enriched in semi-volatile alkali metals. Sulfur
340 was present in all samples, but was enriched in the
341 ultrafine fraction. The high carbon particle com-
342 positions followed similar inorganic component
343 trends as the medium carbon samples, with the
344 obvious exception that these samples contained
345 significantly higher amounts of carbon. For this
346 group, the coarse and fine fractions each con-
347 tained 80% carbon (presumably primarily as char)
348 and the ultrafine fraction contained over 95% car-
349 bon (as soot). The carbon partitioned similarly in

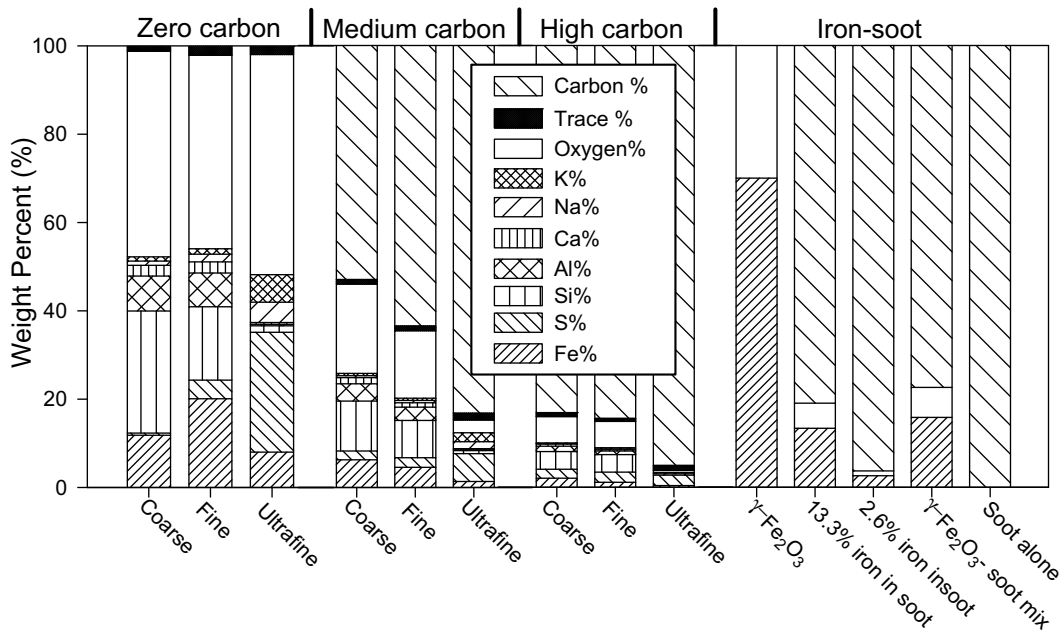


Fig. 1. Bulk composition of size-classified coal combustion ash and pyrolysis residue particles and flame-generated iron-soot particles determined by WD-XRF analysis. Carbon determined by analysis. Composition of iron oxide nanoparticles was estimated based on oxidation form provided by manufacturer.

350 both the medium and high carbon ultrafine samples (~5% OC and ~95% EC). These relatively
 351 low OC values suggest soot-like chemistry with
 352 relatively minor amounts of organic species. The
 353 ethylene derived samples contained only carbon
 354 (soot) and iron (oxide assumed), as per Yang
 355 et al. [11] as shown. The physical mixture of γ -
 356 Fe_2O_3 nanoparticles and flame-formed soot con-
 357 tained 15.8% iron which is similar to the flame-
 358 formed (ferrocene doped) mixture containing
 359 13.3% iron.

361 3.3. Iron and sulfur speciation

362 Examples of the iron Mössbauer and the sulfur
 363 XAFS spectra for selected samples are shown in
 364 Fig. 2 and a summary of results are presented
 365 for the nine particle samples in Fig. 3 for iron
 366 (upper panel) and sulfur (lower panel). The sam-
 367 ple mass for the ultrafine fraction of the zero car-
 368 bon particles was insufficient to allow Mössbauer
 369 analysis. However, previous analysis [13] of a car-
 370 bon free ultrafine samples from a *Utah* coal
 371 showed the iron formed under those conditions
 372 to be γ - Fe_2O_3 . For the zero carbon particles,
 373 the coarse and fine fractions contained all the iron
 374 as either hematite (α - Fe_2O_3) or amorphous Fe^{3+}
 375 in glass. For the medium carbon particles, the iron
 376 appeared as magnetite (Fe_3O_4 and γ - Fe_2O_3) and
 377 several reduced forms of iron. For the high carbon
 378 particles, the iron was present in even more
 379 reduced forms (including metallic iron) in the

coarse and fine fractions suggesting that carbon
 was present in the char. This iron speciation trend
 from the high carbon to zero carbon samples is
 consistent with the study by Huffman et al. [25],
 and undoubtedly reflects the oxidation conditions
 of the combustion and the breakdown and oxida-
 tion of pyrite in the coal, first to iron sulfides
 ($\text{FeS} + \text{Fe}_{1-x}\text{S}$) and metallic phases and then to
 iron oxides (magnetite, Fe_3O_4). Interestingly, only
 the fine medium carbon and high carbon samples
 exhibited carbide phases (Fe_3C) or alloys (austen-
 ite, Fe-C). Such phases did not appear to be present
 in either the corresponding coarse or ultrafine
 samples, and while their formation is rather un-
 usual, it is consistent with the hypothesis that the
 fine fragmentation mode is enriched in extraneous
 pyrite particles. Interestingly, iron appeared
 almost exclusively as amorphous Fe^{3+} in the
 ultrafine fraction, consistent with the oxidation
 state of iron nanoparticles in sooting ethylene
 flames reported by Yang et al. [11], suggesting that
 the sooting ethylene flame can generate similar
 prototype particles at least in regards to iron
 and soot. Iron speciation data for the ferrocene-
 doped ethylene flame samples were not available
 but might be assumed to also consist of Fe_2O_3
 (see Yang et al. [11]).

The sulfur spectra of the three zero carbon
 samples appeared quite different from those of
 the medium carbon and high carbon samples
 and exhibited peaks only at the high end of the
 XAFS energy range that arise from oxidized sul-

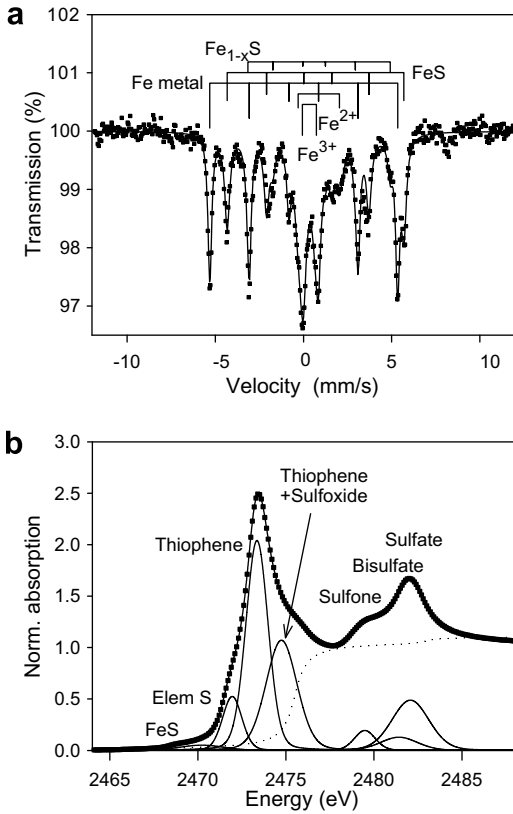


Fig. 2. Spectra of selected samples analyzed by iron Mössbauer and sulfur XAFS spectroscopies. Mössbauer spectrum of high carbon coarse sample (a) is fitted to three magnetic sextets, representing metallic iron and iron sulfides, and two quadrupole doublets representing Fe^{3+} and Fe^{2+} in non-magnetic iron oxides or aluminosilicate glass. A small amount of magnetite, Fe_3O_4 , is also present as indicated by the small peak at about 8 mm/s, but was not fitted. Sulfur XANES spectrum of the high carbon ultrafine sample (b) is deconvoluted to indicate the relative contributions of individual peak components.

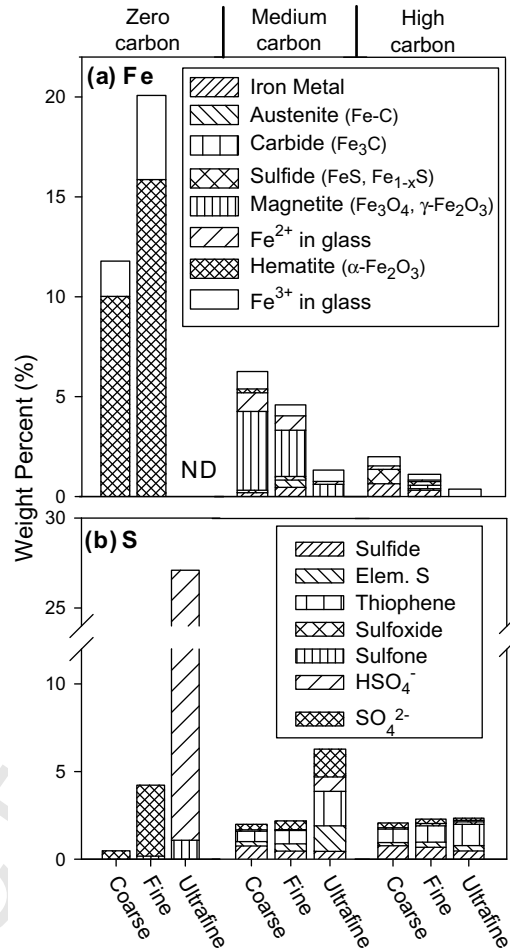


Fig. 3. Summary of (a) iron Mössbauer and (b) sulfur XAFS analysis for nine coal samples (ND, no data).

fur forms; principally sulfate for the coarse and fine fractions and bisulfate for the ultrafine fraction. In contrast, the carbon-containing samples exhibited sulfur XAFS peaks due to reduced sulfur forms, principally organosulfur (thiophene), elemental sulfur, and iron sulfide, as well as peaks for oxidized forms, organosulfone, and sulfate. The sulfur speciation in the high carbon samples was independent of particle size and consisted only of reduced forms of sulfur, present in relatively small fractions compared to the high carbon contents.

3.4. Pulmonary inflammation

Pulmonary inflammation was quantified by the pro-inflammatory cytokine interleukin-6

(IL-6) and the recruitment of inflammatory cell neutrophils in the bronchoalveolar lavage fluid (BALF) at 4 and/or 18 h post-instillation. IL-6 (which is a heat shock protein) was chosen as a marker of inflammatory signaling, because it showed a more sensitive response for lung injury than other cytokines such as MIP-2 and $\text{TNF-}\alpha$. For coal samples, the IL-6 response was greatest at 4 h and the neutrophil response was highest at 18 h and these higher-response data were used for further investigation. For flame-generated iron-soot particles, data from a pilot study indicated that IL-6 and neutrophils were greater at 4 h than 18 h, so the full scale bioassay with five types of particles was conducted only at the 4 h time point. Microalbumin in the BALF was also monitored but showed no significant effects for any of the samples (results not shown). The cytokine and neutrophil results are presented in Fig. 4.

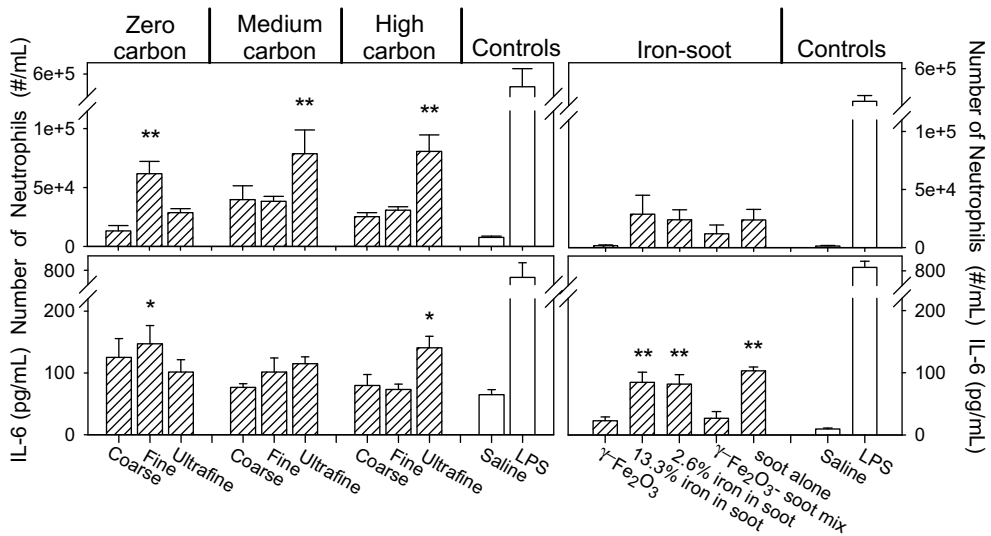


Fig. 4. Indicators of inflammatory response after instillation of 100 µg of different particles in female CD1 mice. Neutrophil and IL-6 concentrations measured in BAL fluid. Neutrophil was measured 18 h post-exposure for the coal test and 4 h for the ethylene flame test. IL-6 was measured 4 h post-exposure for both tests. Statistical difference compared to saline control was indicated as: * $p < 0.05$; ** $p < 0.01$.

447
448
449
450
451
452
453
454
455
456
457
458
459
460
461
462
463
464

3.4.1 Zero carbon particles

Surprisingly, in the absence of carbon, the ultrafine particles were not the most toxic. Compared to the ultrafine and coarse fractions, the influx of neutrophils was significantly higher after exposure to the fine fraction (0.5–2.5 µm) and the corresponding IL-6 response was also elevated, although not significantly (see Fig. 4). This would suggest that the semi-volatile metals and the condensed bisulfate present in the vaporization-nucleation formed ultrafine fraction were less toxic than the fine fraction that contained partially silicated metals with condensed sulfate. The fine sample also contained the largest amounts of silicated Fe³⁺, consistent with the conclusion of Veranth et al. [9], that glassy Fe³⁺ forms of iron are most bio-available to lung tissue in part due to leaching by the alveolar fluid.

465
466
467
468
469
470
471
472
473
474
475
476
477
478
479

3.4.2. Medium and high carbon particles

In the presence of medium and high amounts of carbon, the ultrafine fractions demonstrated the greatest potential for lung injury, especially with neutrophil recruitment, while the IL-6 response was less profound. The neutrophil response to the ultrafine fractions (whose carbon was soot) was significantly greater than for the fine and coarse fractions whose carbon was most likely char. The OC contents of the ultrafine fraction samples were fairly low (~5%), and it is unclear if OC was responsible for the increased toxicity of the ultrafine particles as the OC/EC ratios of the size classified samples (both medium and high carbon) were similar. The ultrafine sam-

ples also contained significantly less iron than the fine and the coarse samples, although the iron speciation was similar. The high carbon ultrafine sample, which contained much less iron, caused little noted difference in toxicity compared to the medium carbon ultrafine sample. Therefore, these data do not support the hypothesis that iron and soot in combination enhance the toxicity of the ultrafine particles. Pulmonary inflammation may correlate with soot carbon (as in Linak et al. [13]), but in these tests the soot concentration in the ultrafine samples did not vary by a sufficient amount (it was always over 80%) to allow extraction of a dependence of inflammation on soot alone. When compared with the zero carbon fine fraction, these ultrafine particles induced neutrophils and IL-6 responses to the same level.

3.4.3. Iron-soot particles

Neutrophil and IL-6 responses to the ethylene flame particles also failed to support the hypothesis that iron plus soot are more toxicologically active than soot alone. Instead, soot alone was at least (if not more) toxic than the flame-formed iron-soot samples. Neutrophils and IL-6 responses induced by soot alone were comparable or higher than those caused by iron-containing soot particles. Among samples containing iron, the toxicity was greater in the order: soot containing 13.3% iron > soot containing 2.6% iron > physical mix of γ-Fe₂O₃ nanoparticles with soot > γ-Fe₂O₃ nanoparticles alone. Especially, IL-6 responses to the flame-generated iron-containing soot particles were significantly greater

480
481
482
483
484
485
486
487
488
489
490
491
492
493
494
495
496
497
498
499
500
501
502
503
504
505
506
507
508
509
510
511
512

as compared to non-flame-generated particles. The toxicity did not vary monotonically with soot content, as we suggested previously [13]. The results for soot alone are also at variance with those of Zhou et al. [26]. The reasons for this are not clear but may be due to different exposure techniques (inhalation vs. instillation) and/or differences in the biological markers used. Instillation was chosen because the small scale of the experimental equipment needed to control the coal fly-ash carbon composition and size classification produced insufficient particle concentrations for whole animal inhalation exposures. Although instillation does not necessarily model the mechanism by which particles reach the respiratory system, it is an accepted method to administer study particles of different toxicity and allows investigating multiple cell types and functions, which is more realistic than cell based assays.

4. Conclusions

A series of specially engineered tests, in which particles were systematically created to have various amounts of carbon and iron from coal combustion, showed that the presence of soot especially in the ultrafine fraction ($<0.5\ \mu\text{m}$) affected pulmonary inflammation. The inflammatory responses were not however associated with total carbon in the coarse and fine samples, since this consisted of both char and soot. Also the tests did not support the hypothesis that the simultaneous presence of iron and carbon in particles might lead to increased pulmonary inflammation. These conclusions were confirmed by additional experiments involving iron-doped sooting ethylene diffusion flames, where the greatest increase in IL-6 production and neutrophil recruitment, two indicators of lung inflammation, occurred for soot particles alone, rather than from flame-formed iron-soot mixtures. Interestingly, a physical mixture of purchased $\gamma\text{-Fe}_2\text{O}_3$ nanoparticles combined with flame-formed soot gave a lower response than the same concentration of iron in flame-formed iron-soot particles.

Mössbauer and XAFS spectroscopies were used to determine the forms of iron and sulfur present in a suite of nine coal samples that represented three combustion conditions (including pyrolysis) and three particle size ranges. Both iron and sulfur exhibited surprisingly complex assemblages of different forms in the carbon-containing samples and simpler assemblages in the ash-only samples. For both elements, a wide range of oxidation states was present in these samples, especially those that contain significant carbon. The zero carbon samples exhibited iron and sulfur in their most oxidized forms, as Fe^{3+} in oxides and other phases, and as sulfate. In the carbon-containing samples, sulfur existed as iron sulfide, ele-

mental sulfur, and thiophenic sulfur, in addition to lesser amounts of sulfate; whereas iron was found in metallic, sulfide and carbide phases, as well as in oxide phases. More specific observations are as follows: (1) bisulfate forms were present in the ultrafine samples, but were lacking in the fine and coarse samples; (2) thiophene sulfur and iron sulfides were most significant in the carbon-containing samples and absent from the zero carbon samples; (3) iron was present as carbide phases only in the fine size fractions of samples containing carbon; and (4) magnetite (\pm maghemite) was only significant in the medium carbon samples. The ability to produce combustion particles with varying components and chemical reactivity is an important step to help understand the relative toxicity of complex combustion products and how the health effects may be related to particular sources of air pollution.

Acknowledgments

Portions of this work were sponsored under P.O. EP06C000237 with J.O.L. Wendt and Contract EP-C-04-023 with ARCADIS G&M Inc. The analytical work performed at the University of Kentucky was supported by a NSF CRAEMS Grant CHE0089133. The authors acknowledge the U.S. Department of Energy for its support of synchrotron facilities in the U.S., Charly King, Daniel Janek, Ha-Na Jang, and Takuya Shinagawa for their help with the drop-tube furnace and ethylene diffusion flame burner experiments, and Mary Daniels and Liz Boykin for their assistance with the toxicity studies. The research has been reviewed by the U.S. EPA National Risk Management Research Laboratory and approved for publication. The contents of this article do not represent Agency policy nor does mention of trade names or commercial products constitute endorsement or recommendation for use.

References

- [1] C.A. Pope, *Am. J. Public Health* 79 (5) (1989) 623–628.
- [2] P.S. Gilmour, D.M. Brown, T.G. Lindsay, P.H. Beswick, W. MacNee, K. Donaldson, *Occup. Environ. Med.* 53 (81) (1996) 7–22.
- [3] J.D. Carter, A.J. Ghio, J.M. Samet, R.B. Devlin, *Toxicol. Appl. Pharmacol.* 146 (1997) 180–188.
- [4] A.J. Ghio, R.B. Devlin, *Am. J. Resp. Crit. Care* 164 (4) (2001) 704–708.
- [5] J.M.S. van Maanen, P.J.A. Borm, A. Knaapen, et al., *Inhal. Toxicol.* 11 (1999) 1123–1141.
- [6] K.R. Smith, J.M. Veranth, J.S. Lighty, A.E. Aust, *Chem. Res. Toxicol.* 11 (1998) 1494–1500.
- [7] K.R. Smith, A.E. Aust, *Chem. Res. Toxicol.* 10 (1997) 828–834.
- [8] D.W. Dockery, C.A. Pope, X. Xu, et al., *New Engl. J. Med.* 329 (1993) 1753–1759.

- 627 [9] J.M. Veranth, K.R. Smith, A.A. Hu, J.S. Lighty, 648
628 A.E. Aust, *Chem. Res. Toxicol.* 13 (2000) 382–389. 649
- 629 [10] J.M. Veranth, K.R. Smith, F. Huggins, A.A. Hu, 650
630 J.S. Lighty, A.E. Aust, *Chem. Res. Toxicol.* 13 651
631 (2000) 161–164.
- 632 [11] G.S. Yang, S. Teague, K. Pinkerton, I.M. Kennedy, 652
633 *Aerosol Sci. Technol.* 35 (2001) 759–766. 653
- 634 [12] H. Jung, B. Guo, C. Anastasio, I.M. Kennedy, 654
635 *Atmos. Environ.* 40 (2006) 1043–1052. 655
- 636 [13] W.P. Linak, J.-I. Yoo, S.J. Wasson, et al., *Proc.* 656
637 *Combust. Inst.* 31 (2007) 1929–1937. 657
- 638 [14] J.M. Veranth, T.H. Fletcher, D.W. Pershing, A.F. 658
639 Sarofim, *Fuel* 79 (9) (2000) 1067–1075. 659
- 640 [15] W.P. Linak, C.A. Miller, W.S. Seames, et al., *Proc.* 660
641 *Combust. Inst.* 29 (2002) 441–447. 661
- 642 [16] W.S. Seames, J.O.L. Wendt, *Proc. Combust. Inst.* 662
643 31 (2007) 2839–2846. 663
- 644 [17] SRI Procedure Manual for the Recommended ARB 664
645 Sized Chemical Sample Method (Cascade 665
646 Cyclones), Report No. SoRI-EAS-86-467, South- 666
647 ern Research Institute, 1986. 667
- [18] R.J. Santoro, H.G. Semerjian, R.A. Dobbins, 668
Combust. Flame 51 (2) (1983) 203–218. 649
- [19] M.H.G. Jacobs, P.J. Vanekeren, C.G. Dekruif, *J.* 650
Chem. Thermodyn. 15 (7) (1983) 619–623. 651
- [20] J. Zhang, J. C.M. Megaridis, *Proc. Combust. Inst.* Q2 652
25 (1994) 593–600. 653
- [21] R. Scholtz, S. Uhlig, *Introduction to X-Ray Fluoro-* 654
rescence (XRF): Guide to XRF Basics, Bruker AXS 655
Inc., Madison, WI, 2006. 656
- [22] T. Shoji, F.E. Higgins, G.P. Huffman, W.P. Linak, 657
C.A. Miller, *Energ. Fuel* 16 (2) (2002) 325–329. 658
- [23] F.E. Huggins, S.V. Vaidya, N. Shah, G.P. Huffman, 659
Fuel Proc. Technol. 35 (3) (1993) 233–257. 660
- [24] G.P. Huffman, S. Mitra, F.E. Huggins, N. Shah, 661
Energ. Fuel 5 (1991) 574–581. 662
- [25] G.P. Huffman, F.E. Huggins, A.A. Levasseur, O. 663
Chow, S. Srinivasachar, A.K. Mehta, *Fuel* 68 664
(1989) 485–490. 665
- [26] Y.-M. Zhou, C.-Y. Zhong, I.M. Kennedy, V.J. 666
Leppert, K.E. Pinkerton, *Toxicol. Appl. Pharm.* 190 667
(2003) 157–169. 668
- 669